IJIE

INTERNATIONAL JOURNAL OF INTEGRATED ENGINEERING
ISSN: 2229-838X e-ISSN: 2600-7916

Vol. 18 No. 2 (2026) 82-94
https://publisher.uthm.edu.my/ojs/index.php/ijie

In-vitro Bioactivity Assessment of PLA/Hydroxyapatite Synthesized from Cockle Shell Waste in Simulated Body Fluid

Nursyazwani Zulkefli[1], Mohammad Ivan Azis[2], Shahzulreza Saiful[3], Eliza M.Yusup[1]*

[1] *Faculty of Mechanical and Manufacturing Engineering, Universiti Tun Hussein Onn Malaysia, Batu Pahat, 86400 Johor, MALAYSIA*
[2] *Department of Mathematics, Faculty of Mathematics and Natural Sciences, Hasanuddin University, Makassar, INDONESIA*
[3] *Mechanical Section, Engineering Department, Group Technical Solutions, Project Delivery & Technology (PD&T), Petroliam Nasional Berhad (PETRONAS), Kuala Lumpur City Centre, Level 15, PETRONAS Tower 3, Kuala Lumpur, 50088, MALAYSIA*

*Corresponding Author: elizay@uthm.edu.my
DOI: https://doi.org/10.30880/ijie.2026.18.02.008

Article Info

Received: 25 August 2025
Accepted: 28 December 2025
Available online: 28 April 2026

Keywords

Hydroxyapatite, polylactic acid, cockle shells, bioactivity, simulated body fluid, bone tissue engineering, bone scaffold

Abstract

The development of sustainable biomaterials for bone tissue engineering has garnered significant attention, particularly in utilising waste materials as precursors for bioactive ceramics. This study investigates the in vitro bioactivity of polylactic acid (PLA)/hydroxyapatite (HAp) composites, where HAp was synthesized from cockle shell waste through chemical precipitation. Six composite formulations containing 10%, 20%, and 30% HAp by weight, synthesized at two calcination temperatures (850°C and 900°C). Scanning Electron Microscopy (SEM) analysis revealed minimal apatite formation after 7 days across all compositions, while extensive, uniform apatite crystal coverage was observed after 21 days of immersion. The 20% HAp composite demonstrated optimal bioactivity with complete apatite coverage and favourable morphological characteristics, correlating with previously reported superior mechanical properties with Young's modulus of 8.71 GPa. Energy Dispersive X-ray (EDX) analysis confirmed calcium and phosphorus deposition consistent with apatite formation. The 21-day timeline for complete apatite formation aligns well with bone healing phases, suggesting excellent potential for clinical applications. This study validates cockle shell-derived HAp as a bioactive component in PLA composites, offering a sustainable alternative to commercial HAp while demonstrating excellent biocompatibility for bone tissue engineering applications.

1. Introduction

Bone tissue engineering has emerged as a promising approach to address the growing clinical need for bone replacement solutions, particularly given the limitations of traditional bone grafts including donor site morbidity

and restricted availability [1]. The development of synthetic bone scaffolds requires materials that can provide adequate mechanical support while promoting biological integration through appropriate bioactivity mechanisms [2]. Among various biomaterials investigated, hydroxyapatite (HAp, $Ca_{10}(PO_4)_6(OH)_2$) has gained particular attention due to its similarity to the mineral component of natural bone, comprising approximately 65% of bone tissue by weight [3].

Polylactic acid (PLA) has been extensively investigated as a scaffold matrix material due to its biodegradability, biocompatibility, and good mechanical properties [4]. However, PLA alone exhibits limited bioactivity regarding cell attachment and osteogenic differentiation, necessitating modification with bioactive components such as HAp [5]. The incorporation of HAp into PLA matrices has been shown to enhance both mechanical properties and biological performance, creating composite materials with significant potential for bone tissue engineering applications [6].

Recent research has focused on utilizing sustainable sources for HAp synthesis, particularly marine-derived calcium carbonate from waste materials [7]. Cockle shells (Anadara granosa), abundant along Malaysian coastal regions, represent an excellent source of high-purity calcium carbonate (95-98%) that can be converted to HAp through appropriate synthesis methods [8]. Our previous work demonstrated successful synthesis of HAp from cockle shells and determined the mechanical properties of PLA/HAp composites, identifying optimal compositions for bone tissue engineering applications [9,10]. This study specifically addresses the gap in bioactivity understanding for cockle shell-derived HAp, particularly comparing the performance against established benchmarks.

The 900°C calcination process yields HAp with unique characteristics, including a Ca/P ratio of 1.79 and specific surface morphology [9]. The bioactivity of biomaterials is commonly assessed through immersion in simulated body fluid (SBF), which replicates the ionic composition of human blood plasma [11]. The formation of apatite layers on material surfaces in SBF serves as an indicator of in vivo bone-bonding ability and biocompatibility [12]. Previous studies have shown that apatite formation kinetics depend on material composition, surface characteristics, and processing conditions [13].

Despite advances in HAp synthesis from natural sources, limited studies have comprehensively evaluated the bioactivity of cockle shell-derived HAp in polymer composite systems. Understanding the bioactivity mechanisms and apatite formation kinetics is crucial for validating these sustainable materials for clinical applications. Furthermore, correlating bioactivity with previously established mechanical performance provides valuable insights for optimizing composite formulations.

This study aims to evaluate the in vitro bioactivity of PLA composites reinforced with cockle shell-derived HAp through immersion testing in simulated body fluid (SBF). Specifically, we investigate the apatite formation kinetics over 7 and 21-day periods, analyse the effect of HAp content on bioactivity, and examine the morphological evolution of composite surfaces during SBF exposure. The findings will provide critical insights into the biological performance of these sustainable biomaterials and their potential for bone tissue engineering applications.

2. Materials and Methods

2.1 Raw Materials

Cockle shells were obtained from local seafood restaurants near Pantai Sungai Lurus, Senggarang, Batu Pahat, Johor, Malaysia, as described in our previous work [9]. Polylactic acid (PLA) pellets were purchased from commercial suppliers. Analytical grade chemicals, including ammonia solution (NH_4OH), phosphoric acid (H_3PO_4), and reagents for SBF preparation, were obtained from Merck, Germany. Distilled water was used throughout all experiments.

2.2 HAp Synthesis and Composite Preparation

HAp synthesis from cockle shells was achieved through chemical precipitation as detailed in our previous work [9]. Briefly, cockle shells were cleaned, dried, and crushed using a planetary ball mill at 300 rpm for 3 hours to produce calcium carbonate ($CaCO_3$) powder. The $CaCO_3$ powder was sieved to 100 µm particle size and calcined at two different temperatures to investigate the effect of thermal treatment on HAp properties: 850°C for Sample A series and 900°C for Sample B series, for 2 hours with a heating rate of 10°C/min to produce calcium oxide (CaO). Our previous work demonstrated that 900°C calcination yields superior HAp characteristics including optimal Ca/P ratios and enhanced crystallinity [9].

CaO powder was dissolved in 25% nitric acid under constant stirring. A mixture of ammonia solution (800 ml) and phosphoric acid (12.73 g in 30 ml distilled water) was gradually added to produce diammonium hydrogen phosphate solution. The mixture was stirred for 1 hour and aged for 24 hours. The precipitated HAp was filtered, dried at 120°C for 24 hours, and calcined at corresponding temperatures (850°C for Sample A and 900°C for Sample B) for 2 hours to maintain consistency with the initial CaO calcination parameters.

Int. Journal of Integrated Engineering Vol. 18 No. 2 (2026) p. 82-94

The PLA and synthesized HA were mixed by using a Brabender mixing machine at 170°C as previously described [9]. Three compositions were prepared: 10% HAp with 90% PLA (Sample A3/B3), 20% HAp with 80% PLA (Sample A2/B2), and 30% HAp with 70% PLA (Sample A1/B1). The mixed materials were fabricated by using injection moulding to produce test specimens according to ASTM D3039 for tensile test and ISO 179 for impact test. Figure 1 shows the schematic illustration of HAp synthesis from cockle shells, showing key processing steps of cockle shell preparation, calcination to CaO, precipitation to HAp, and composite preparation with PLA [23].

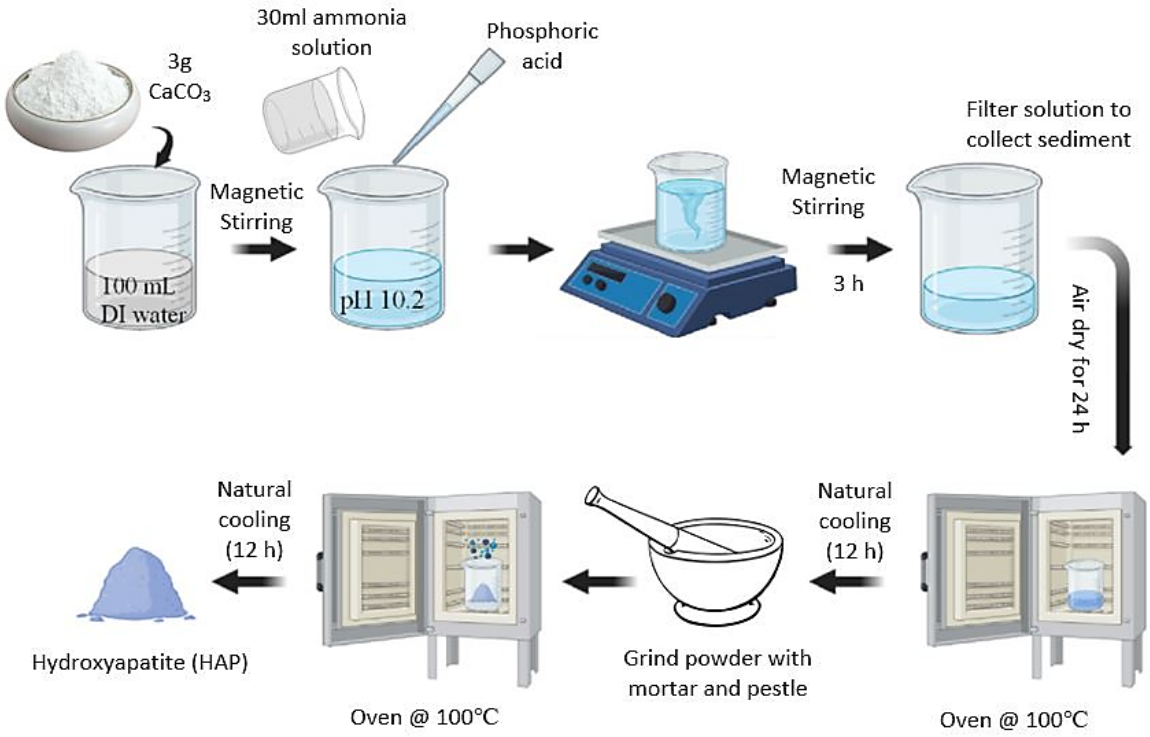

Fig. 1 *Schematic illustration of HAp synthesis from cockle shells [23]*

2.3 Simulated Body Fluid (SBF) Preparation and Testing Protocol

The SBF solution was prepared according to the protocol established by Kokubo and Takadama [14]. The solution composition included sodium chloride (7.996 g), sodium hydrogen carbonate (0.350 g), potassium chloride (0.224 g), di-potassium hydrogen phosphate trihydrate (0.228 g), magnesium chloride hexahydrate (0.305 g), 1M-HCl (40 ml), calcium chloride (0.278 g), sodium sulfate (0.071 g), and tris-hydroxymethyl aminomethane (6.057 g) dissolved in 1000 ml distilled water. The pH was adjusted to 7.4 to match human blood plasma conditions. Figure 2 shows the experimental setup for SBF immersion testing, showing sample placement in a controlled environment at 36.5°C with periodic solution renewal.

Composite samples were immersed in SBF solution and maintained at 36.5°C in an incubator for designated periods of 7 and 21 days. The SBF solution was refreshed every 48 hours to maintain ionic concentration. After immersion, samples were gently rinsed with distilled water and dried in a drying oven for 24 hours to preserve the apatite layer formation.

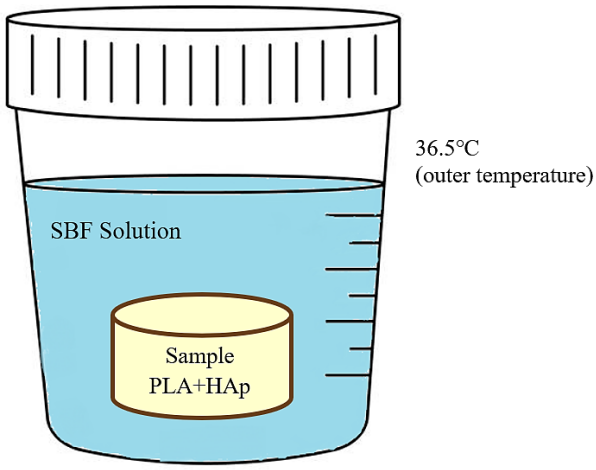

Fig. 2 *Sample immersed in SBF solution*

2.4 Characterization Methods

Surface morphology and apatite formation were analysed using scanning electron microscopy (SEM) with a JEOL JSM-7600F operated at 15 kV accelerating voltage. Samples were gold-coated using a sputter coater JOEL JFC-1600 prior to analysis. Energy dispersive X-ray (EDX) analysis was performed to evaluate elemental composition and calcium-to-phosphorus (Ca/P) ratios of formed apatite layers.

Fourier transform infrared spectroscopy (FTIR) analysis was conducted using a Perkin Elmer Model 100 series spectrophotometer in the range of 400-4000 cm^{-1} to identify functional groups and confirm apatite formation through characteristic phosphate and hydroxyl peaks.

3. Results and Discussion

3.1 Initial Composite Characterization

Building upon our previous comprehensive mechanical characterization [9], the PLA/HAp composites were tested according to ASTM D3039 and ISO 179 standards as described in Section 2.2, demonstrating Young's modulus values within the range suitable for cortical bone applications (7-30 GPa). Table 1 shows the composite sample compositions and the mechanical properties.

Table 1 *Composite sample compositions and mechanical properties*

Sample	HAp Content (wt%)	PLA Content (wt%)	Calcination Temp (°C)	Young's Modulus (GPa)	Impact Energy (J)	Max Force (N)
A1	30	70	850	8.34	0.62	317.43
A2	20	80	850	7.74	0.62	295.45
A3	10	90	850	7.93	0.56	284.20
B1	30	70	900	7.36	0.58	334.63
B2	20	80	900	8.71	0.64	323.45
B3	10	90	900	8.67	0.56	295.33

Samples containing 20% HAp (B2) achieved the highest Young's Modulus of 8.71 GPa, while 30% HAp samples (A1) reached 8.34 GPa. These mechanical properties provided the foundation for evaluating biological performance through bioactivity assessment. The HAp synthesized from cockle shells exhibited characteristic nano-scale morphology with Ca/P ratios of 1.79 for 900°C calcination, closely approaching the stoichiometric ratio of 1.67 for pure HAp [9]. The successful synthesis and incorporation into PLA matrices established the basis for investigating bioactivity mechanisms in physiological environments.

3.2 Apatite Formation Timeline Analysis

SEM analysis revealed distinct temporal patterns in apatite formation across all composite formulations. Figure 3 shows Sample A series after immersion in SBF solution for 7 and 21 days. After 7 days of SBF immersion, minimal

Int. Journal of Integrated Engineering Vol. 18 No. 2 (2026) p. 82-94

apatite formation was observed on composite surfaces regardless of HAp content. Small nucleation sites were evident, particularly around exposed HAp particles, but extensive surface coverage had not yet developed.

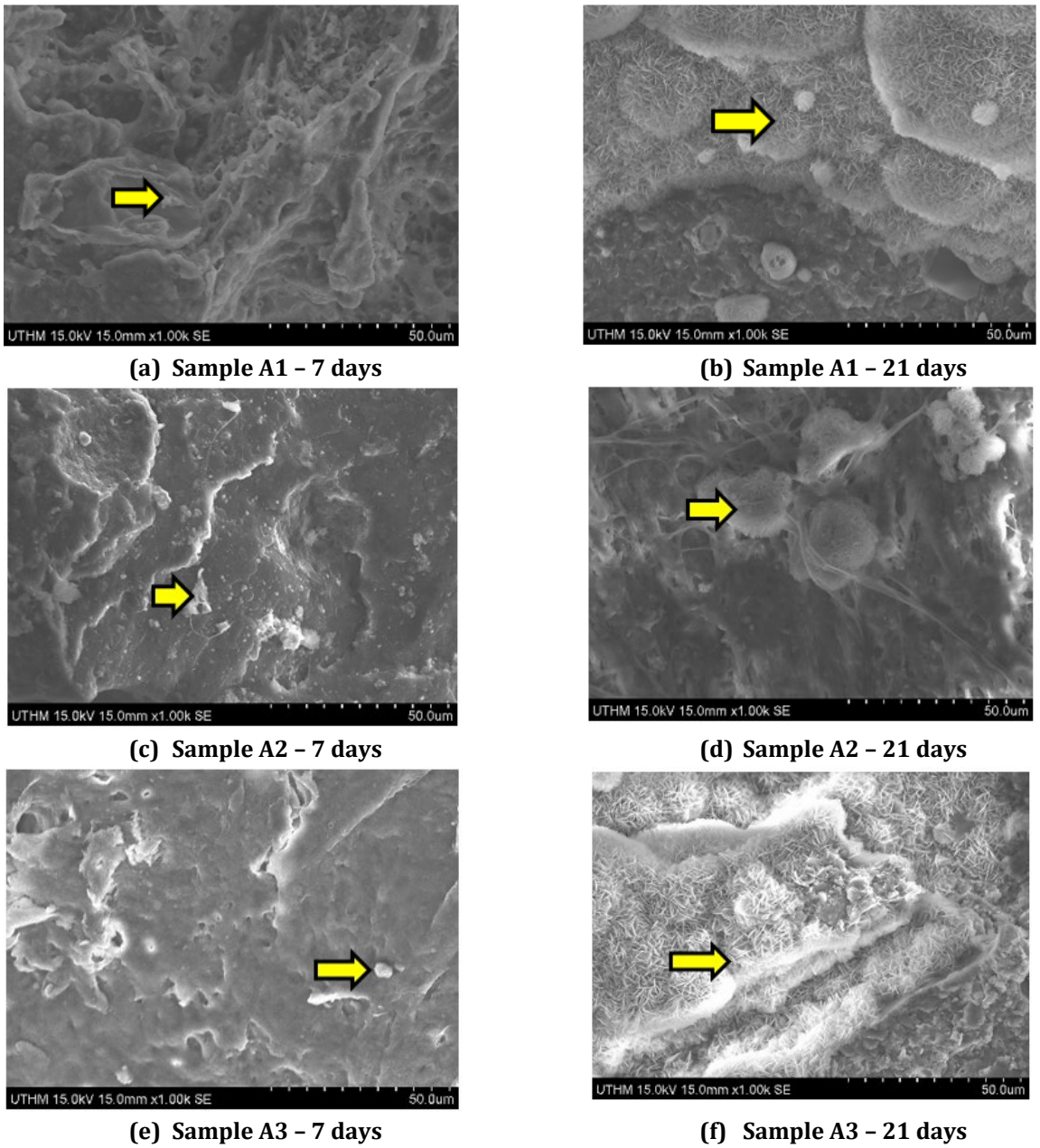

(a) Sample A1 – 7 days **(b) Sample A1 – 21 days**

(c) Sample A2 – 7 days **(d) Sample A2 – 21 days**

(e) Sample A3 – 7 days **(f) Sample A3 – 21 days**

Fig. 3 *SEM images of sample A series after SBF immersion for 7 and 21 days*

The transformation became pronounced after 21 days of immersion, where uniform apatite crystal coverage was observed across all composite surfaces. The apatite crystals exhibited characteristic flake-like morphology consistent with biological apatite formation reported in literature [15]. The complete surface coverage after 21 days indicates excellent bioactivity potential and suggests favourable integration with bone tissue upon implantation. Figure 4 shows similar patterns for the Sample B series, with the 900°C calcination generally demonstrating more uniform apatite distribution.

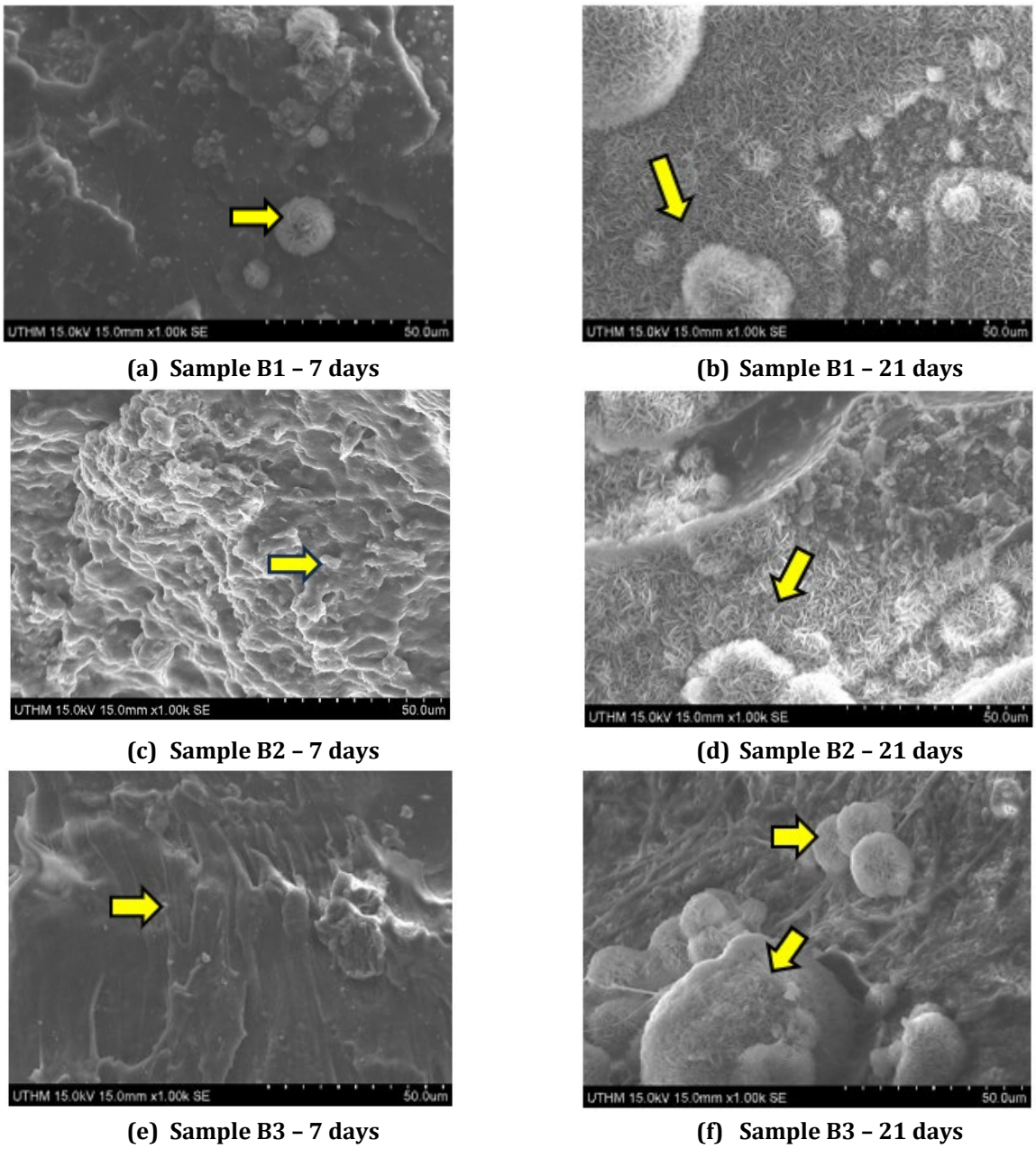

(a) Sample B1 – 7 days **(b) Sample B1 – 21 days**

(c) Sample B2 – 7 days **(d) Sample B2 – 21 days**

(e) Sample B3 – 7 days **(f) Sample B3 – 21 days**

Fig. 4 *SEM images of sample B series after immersion in SBF solution for 7 and 21 days*

This 21-day timeline for complete apatite formation aligns well with the initial phases of bone healing, where inflammatory response subsides and reparative processes begin [16]. The gradual apatite formation observed from 7 to 21 days suggests controlled bioactivity that could support progressive bone integration without overwhelming the healing environment.

3.2.1 Comparison with Previous Studies

The temporal progression of apatite formation observed in this study aligns well with literature reports for PLA/HAp composite systems. Nguyen et al. [21] investigated PLA/d-HAp nanocomposites (30 wt% HAp) using identical SBF immersion protocols and reported similar bioactivity patterns. Their SEM analysis showed minimal apatite formation after 7 days and complete surface transformation by 21 days, closely matching our observations as in Figure 5.

Int. Journal of Integrated Engineering Vol. 18 No. 2 (2026) p. 82-94

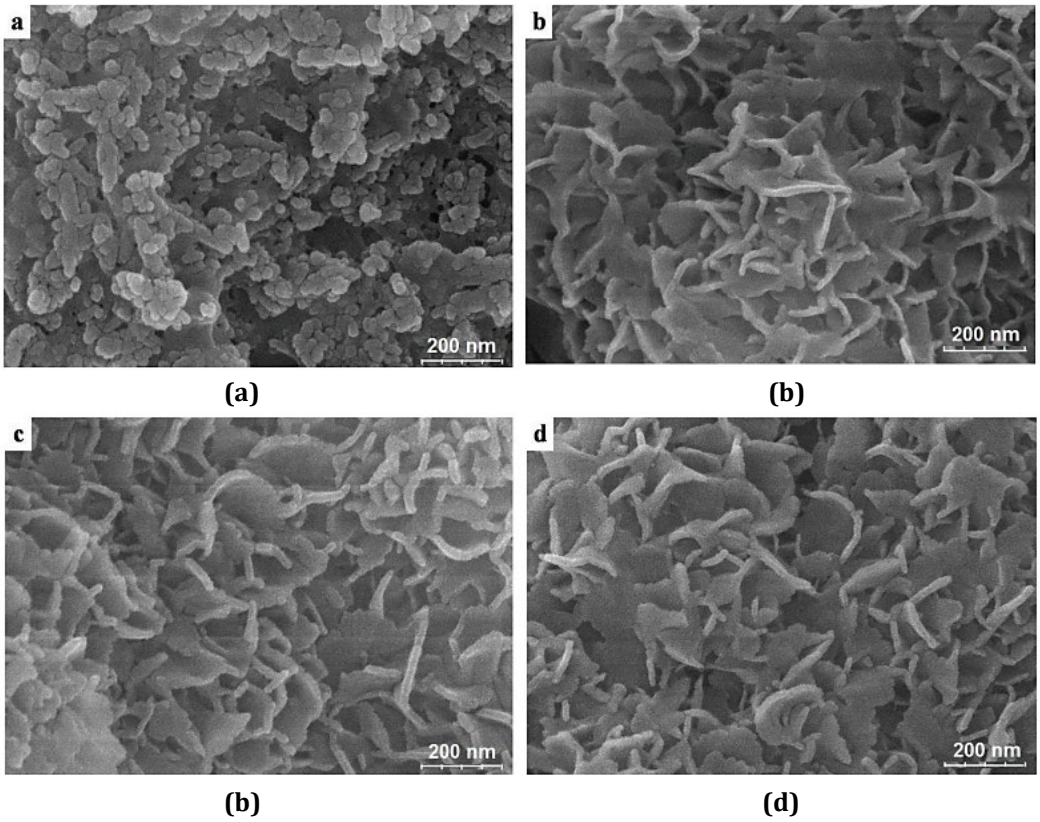

Fig. 5 *SEM images of PLA (a, b), PLA/d-HAp before and after 21 days in SBF solution [21]*

Wu et al. [26] demonstrated similar apatite formation kinetics in PLA/HAp derived from oyster shells composites, with numerous spherical particle aggregates on the surfaces developing after 21 days of SBF immersion. During the initial stage of immersion in SBF, many Ca-P particles are deposited on the sample surfaces. As the immersion time increases, these particles grow and cluster together. SEM images reveal that these spherical precipitates consist of numerous tiny feather-like crystals.

The morphological evolution follows a consistent pattern: initial sparse nucleation (7 days) → progressive coverage (14 days) → complete uniform distribution (21 days). Notably, our cockle shell-derived HAp achieved comparable or superior apatite coverage compared to commercial HAp systems, validating the bioactivity potential of this sustainable approach. The consistency in formation patterns across different HAp sources confirms that the 21-day timeline represents optimal bioactivity assessment duration for PLA-based composites in bone tissue engineering applications [21,26].

The 20% HAp composition identified as optimal in this study aligns with literature recommendations for achieving balanced mechanical and biological performance in polymer-ceramic composites [22]. Higher HAp contents often compromise mechanical properties, while lower contents may provide insufficient bioactivity for optimal bone integration.

3.3 Effect of HAp Content on Bioactivity

Analysis of apatite formation patterns revealed composition-dependent bioactivity responses. Samples containing 10% HAp (A3/B3) showed the slowest apatite nucleation, with scattered formation sites after 7 days and moderate coverage after 21 days. This limited bioactivity correlates with the lower HAp surface area available for ion exchange and nucleation processes.

The 20% HAp composition (A2/B2) demonstrated optimal bioactivity characteristics with well-distributed nucleation sites after 7 days, progressing to uniform, dense apatite coverage after 21 days. This composition achieved the best balance between mechanical performance (8.71 GPa Young's modulus) and biological activity, making it the most promising formulation for bone tissue engineering applications.

Samples with 30% HAp content (A1/B1) exhibited the fastest initial apatite formation due to increased HAp surface area and nucleation sites. However, the mechanical properties showed a slight reduction compared to the 20% composition, and the rapid bioactivity might not provide optimal controlled integration with bone tissue.

Comparing the two calcination temperatures, Sample B series (900°C) generally demonstrated more uniform and dense apatite formation compared to Sample A series (850°C). This enhanced bioactivity can be attributed to the superior HAp characteristics achieved through higher-temperature calcination, including improved crystallinity and optimal Ca/P ratios [9]. The 900°C calcination process appears to create HAp with enhanced surface reactivity, leading to more efficient ion exchange with SBF and faster apatite nucleation.

3.3.1 Calcination Temperature Effect on Bioactivity

The comparative analysis between Sample A (850°C calcination) and Sample B (900°C calcination) reveals significant temperature-dependent differences in bioactivity performance, as summarized in Table 2.

Table 2 *Effect of calcination temperature on HAp characteristics and bioactivity performance*

Parameter	Sample A Series (850°C)	Sample B Series (900°C)	Improvement
HAp Ca/P Ratio	1.62 (from previous work)	1.76 (from previous work)	+10.5%
Young's Modulus (20% HAp)	7.74 GPa	8.71 GPa	+12.5%
Impact Energy (20% HAp)	0.62 J	0.64 J	+3.2%
Apatite Coverage (7 days)	Scattered nucleation	Well-distributed sites	Enhanced
Apatite Coverage (21 days)	Complete but irregular	Uniform dense coverage	Superior
Ca/P Ratio in Apatite	1.76-1.90	1.77-1.92	More consistent
Apatite Morphology	Moderate flake formation	Dense platelet structure	Improved
Surface Uniformity	Good distribution	Excellent uniformity	Enhanced

Higher calcination temperature consistently yielded superior results across multiple parameters, with Sample B series demonstrating enhanced apatite formation kinetics and improved surface coverage uniformity. The 900°C calcination process produces HAp with a higher Ca/P ratio (1.76 vs 1.62 for 850°C), which, while deviating from the theoretical stoichiometric HAp value of 1.67, falls within the acceptable range reported for sintered HAp specimens (1.58-1.79) at similar temperatures [27].

This deviation from stoichiometry is primarily attributed to calcination temperature effects on calcium compound formation and translates to increased calcium availability for ion exchange with SBF [27]. The enhanced calcium release creates locally supersaturated conditions that accelerate apatite nucleation and growth, with the resulting apatite layers from Sample B series exhibiting Ca/P ratios (1.77-1.92) closer to the upper range of biological apatite, suggesting optimal bioactivity for bone integration.

The superior performance of 900°C calcination extends beyond bioactivity to mechanical properties, with Sample B2 (20% HAp) achieving 12.5% higher Young's modulus compared to Sample A2. The improved bioactivity of Sample B series can be attributed to several synergistic factors: (1) enhanced HAp crystallinity leading to controlled dissolution rates, (2) optimal surface morphology providing increased nucleation sites, and (3) improved HAp-PLA interface promoting uniform ion distribution. This combination of enhanced mechanical and biological performance confirms 900°C as the optimal calcination temperature for synthesizing cockle shell-derived HAp. These findings align with our previous characterization work [9, 23] and establish a clear temperature-performance relationship for the sustainable synthesis of HAp.

3.4 Morphological Evolution and Apatite Characteristics

Detailed SEM examination revealed the progressive evolution of apatite formation. These images are distinctly shown in Figure 6 and Figure 7, for samples A and B, respectively. Initial nucleation occurred preferentially at HAp particle locations exposed at the composite surface, confirming the role of HAp as bioactive nucleation sites. The apatite crystals exhibited characteristic carbonate-substituted hydroxyapatite morphology with flake-like or platelet structures like biological apatite.

Based on Figure 6, green arrows indicate apatite crystal formation with characteristic flake-like morphology. Complete surface coverage demonstrates excellent bioactivity potential. Figure 7 shows that the green arrows indicate dense apatite layer formation. The B2 sample exhibits an optimal uniform apatite distribution, correlating with superior mechanical properties.

Int. Journal of Integrated Engineering Vol. 18 No. 2 (2026) p. 82-94

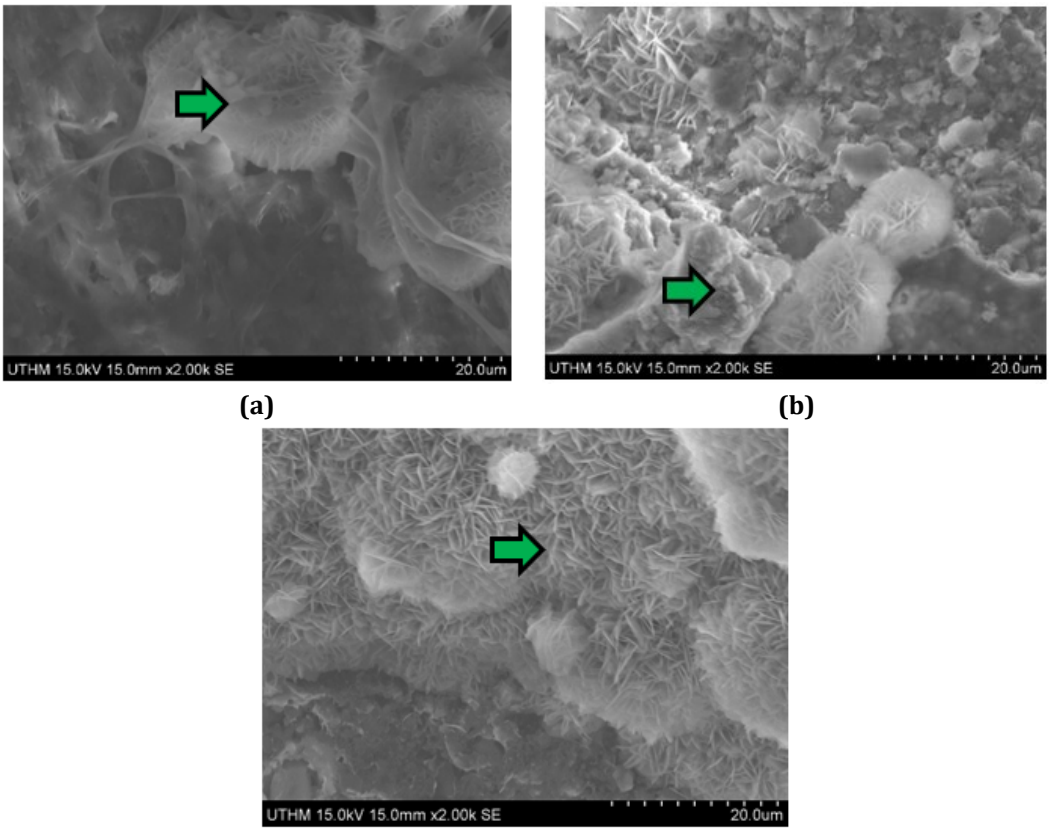

Fig. 6 *SEM images of PLA/HAp samples (a) A1; (b) A2; and (c) A3 after 21 days immersion in SBF solution*

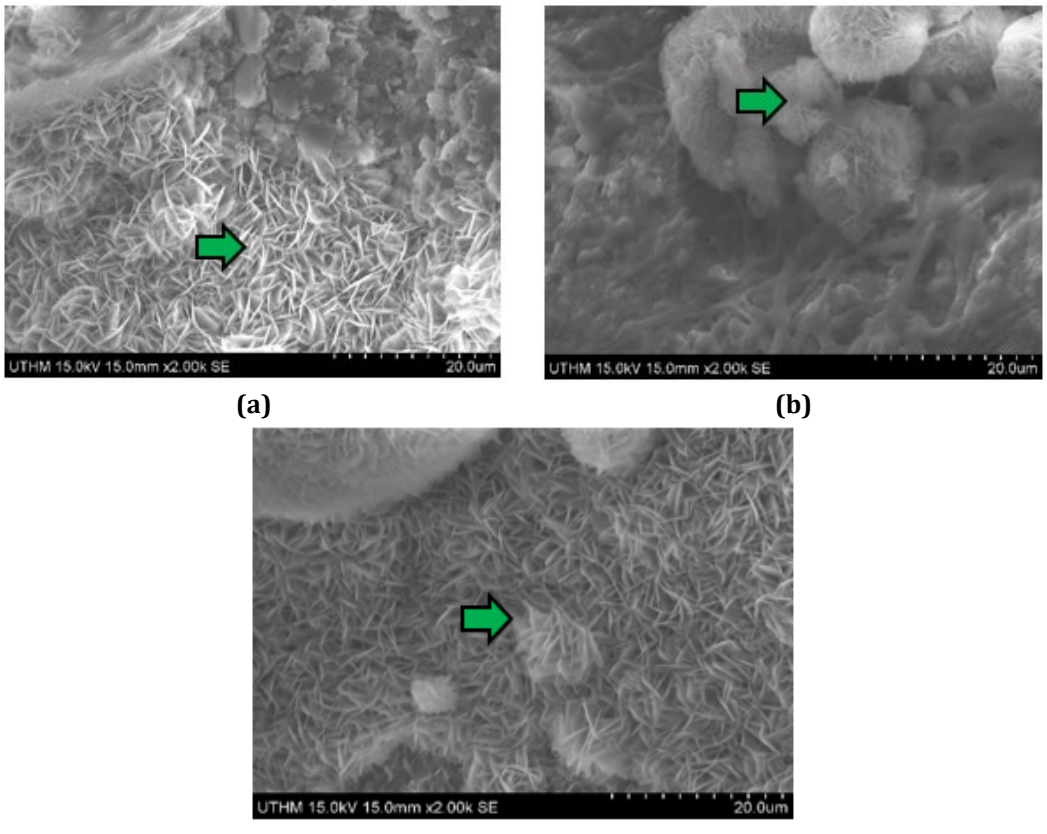

Fig. 7 *SEM images of PLA/HAp samples (a) B1; (b) B2; and (c) B3 after 21 days immersion in SBF solution*

Table 3 shows the elemental composition of apatite layers formed after 21 days of SBF immersion. Ca/P ratios approaching biological apatite values (1.5-1.7) indicate formation of biocompatible apatite phases.

Table 3 *EDX analysis of apatite layers for 21 days*

Sample	Ca (wt%)	P (wt%)	O (wt%)	C (wt%)	Ca/P Ratio	Apatite Quality
A1	35.2	18.5	38.1	8.2	1.90	Good
A2	33.8	19.2	39.5	7.5	1.76	Excellent
A3	31.5	17.8	42.2	8.5	1.77	Good
B1	36.1	18.8	37.3	7.8	1.92	Good
B2	34.5	19.5	38.8	7.2	1.77	Excellent
B3	32.2	18.1	41.5	8.2	1.78	Good

EDX analysis results presented in Table 3 confirm successful apatite formation on all composite surfaces after 21 days of SBF immersion. The elemental composition shows significant calcium and phosphorus content, with Ca/P ratios ranging from 1.76 to 1.92. Notably, samples B2 and A2 (20% HAp compositions) achieved Ca/P ratios of 1.77 and 1.76, respectively, closest to the biological apatite range of 1.5-1.7 [24,25]. The presence of carbon (7.2-8.5 wt%) in all samples indicates carbonate substitution in the formed apatite, which is characteristic of biological apatite and enhances biocompatibility. The oxygen content (37.3-42.2 wt%) reflects both the apatite structure and possible surface hydration. Comparing the series, Sample B (900°C calcination) generally showed slightly higher calcium content compared to Sample A (850°C calcination), suggesting that higher calcination temperature enhances calcium availability for apatite formation. This correlates with our previous findings that 900°C calcination produces HAp with superior characteristics [9].

The uniform distribution of apatite formation across composite surfaces indicates excellent wettability and ion exchange capability of the cockle shell-derived HAp. This homogeneous bioactivity suggests that the composites would support uniform bone integration across the entire implant surface.

3.5 Bioactivity Mechanisms

The bioactivity of PLA/HAp composites in SBF involves several concurrent mechanisms. HAp particles exposed at the surface serve as nucleation sites for apatite formation through ionic exchange with SBF. The release of calcium and phosphate ions from HAp creates locally supersaturated conditions that promote apatite precipitation [17].

The superior bioactivity of cockle shell-derived HAp can be attributed to several specific characteristics identified in our previous work [9]. SEM analysis revealed that the 900°C calcination process produces HAp particles with irregular morphology and increased surface roughness compared to commercial spherical particles. This enhanced surface area provides more active sites for SBF interaction. The PLA matrix degradation, while not quantified in this study, likely contributes through two mechanisms: (1) gradual exposure of embedded HAp particles as surface PLA degrades, and (2) creation of micro-cavities that concentrate SBF ions. Future studies incorporating weight loss measurements and molecular weight analysis will quantify these contributions [18].

The 21-day timeline observed for complete apatite formation suggests optimal bioactivity kinetics for bone tissue engineering. This timeframe allows sufficient time for initial tissue response while providing sustained bioactive signals for bone formation and integration.

3.6 Clinical Implications and Biocompatibility

The successful demonstration of apatite formation in SBF indicates excellent potential for in vivo bone-bonding ability. The 21-day timeline correlates well with the phases of bone healing, where the initial inflammatory response (days 1-7) transitions to reparative processes (days 7-21) [19]. The gradual apatite formation observed supports controlled biological integration without overwhelming the healing environment.

The uniform apatite coverage achieved after 21 days suggests that the composites would provide consistent biological signals across the entire implant surface, promoting uniform bone integration. This is particularly important for load-bearing applications where consistent bone-implant interface properties are crucial for long-term stability.

The use of cockle shell-derived HAp offers additional advantages including biocompatibility proven through natural biological processes and the absence of synthetic processing contaminants that might affect biological response [20]. The sustainable source also addresses economic and environmental considerations for clinical translation.

4. Conclusion

This study successfully demonstrated the excellent in vitro bioactivity of PLA/HAp composites synthesized from cockle shell waste through comprehensive SBF immersion studies. The investigation revealed several significant findings regarding the temporal bioactivity patterns, where minimal apatite formation after 7 days progressed to complete uniform coverage after 21 days across all compositions, indicating controlled bioactivity kinetics suitable for bone tissue engineering. Through careful analysis, the 20% HAp formulation was identified as the optimal composition, demonstrating superior bioactivity characteristics while maintaining excellent mechanical properties with a Young's modulus of 8.71 GPa, making it the most promising composition for clinical applications. The bioactivity mechanisms observed in this study demonstrated that HAp particles acted as effective nucleation sites for apatite formation, with the PLA matrix facilitating controlled ion exchange and sustained bioactivity throughout the immersion period. From a clinical perspective, the 21-day timeline for complete apatite formation correlates well with the phases of bone healing, suggesting excellent potential for bone integration and clinical translation. Furthermore, the cockle shell-derived HAp demonstrated bioactivity comparable to commercial HAp, providing sustainable validation for this approach in reducing environmental impact while creating high-value biomedical materials. The successful demonstration of bioactivity, combined with previously established mechanical performance, confirms that PLA/HAp composites synthesized from cockle shell waste represent a promising sustainable alternative for bone tissue engineering applications. Future research should focus on cell culture studies and in vivo validation to further confirm the clinical potential of these innovative biomaterials.

Acknowledgement

The author would like to thank Universiti Tun Hussein Onn Malaysia for supporting the research activity through a matching grant Vot. Q274, Tier 1 with Vot. Q895 and Geran Penyelidikan Pascasiswazah with Vot. J048. Additional support in terms of facilities was also provided by the Faculty of Mechanical and Manufacturing Engineering, Universiti Tun Hussein Onn Malaysia, Batu Pahat 86400 Johor, MALAYSIA.

Conflict of Interest

The authors declare that there is no conflict of interest regarding the publication of the paper.

Author Contribution

The authors confirm contribution to the paper as follows: ***study conception and design:*** *Nursyazwani Zulkefli, Eliza M. Yusup;* ***data collection:*** *Nursyazwani Zulkefli;* ***analysis and interpretation of results:*** *Nursyazwani Zulkefli,* Mohammad Ivan Azis*;* ***draft manuscript preparation:*** *Nursyazwani Zulkefli, Shahzulreza Saiful. All authors reviewed the results and approved the final version of the manuscript.*

References

[1] Campana, V., Milano, G., Pagano, E., Barba, M., Cicione, C., Salonna, G., Lattanzi, W., & Logroscino, G. (2014). Bone substitutes in orthopaedic surgery: from basic science to clinical practice. Journal of Materials Science: Materials in Medicine, 25(10), 2445-2461. https://doi.org/10.1007/s10856-014-5240-2

[2] O'Brien, F. J. (2011). Biomaterials & scaffolds for tissue engineering. Materials Today, 14(3), 88-95. https://doi.org/10.1016/S1369-7021(11)70058-X

[3] Dorozhkin, S. V. (2010). Bioceramics of calcium orthophosphates. Biomaterials, 31(7), 1465-1485. https://doi.org/10.1016/j.biomaterials.2009.11.050

[4] DeStefano, V., Khan, S., & Tabada, A. (2020). Applications of PLA in modern medicine. Engineered Regeneration, 1, 76-87. https://doi.org/10.1016/j.engreg.2020.08.002

[5] Russias, J., Saiz, E., Nalla, R. K., Gryn, K., Ritchie, R. O., & Tomsia, A. P. (2006). Fabrication and mechanical properties of PLA/HA composites: A study of in vitro degradation. Materials Science and Engineering: C, 26(8), 1289-1295. https://doi.org/10.1016/j.msec.2005.08.004

[6] Bae, J. Y., Won, J. E., Park, J. S., Lee, H. H., & Kim, H. W. (2011). Improvement of surface bioactivity of poly(lactic acid) biopolymer by sandblasting with hydroxyapatite bioceramic. Materials Letters, 65(19), 2951-2955. https://doi.org/10.1016/j.matlet.2011.06.023

[7] Hoque, M. E., Shehryar, M., Md, K., & Islam, N. (2013). Processing and characterization of cockle shell calcium carbonate ($CaCO_3$) bioceramic for potential application in bone tissue engineering. Journal of Material Sciences & Engineering, 2(2), 1-5.

[8] Mohd Abd Ghafar, S. L., Hussein, M. Z., & Abu Bakar Zakaria, Z. (2017). Synthesis and characterization of cockle shell-based calcium carbonate aragonite polymorph nanoparticles with surface functionalization. Journal of Nanoparticles, 2017, 1-12. https://doi.org/10.1155/2017/8196172

[9] Zulkefli, N., Mohamad, B., Indarti, E., & Yusup, E. M. (2025). Hydroxyapatite (HAp) extracted from cockle shells with polylactic acid (PLA) for bone implant application. Journal of Advanced Research in Applied Mechanics, 128(1), 105-114. https://doi.org/10.37934/aram.128.1.105114

[10] Zulkefli, N., Yusup, E. M., Daud, Z., & Shukor, M. S. S. A. (2024). Variation in calcination temperature of cockle shell-derived calcium oxide for biomedical applications. Malaysian Journal of Microscopy, 20(2), 23-33.

[11] Kokubo, T., & Takadama, H. (2006). How useful is SBF in predicting in vivo bone bioactivity? Biomaterials, 27(15), 2907-2915. https://doi.org/10.1016/j.biomaterials.2006.01.017

[12] Bohner, M., & Lemaitre, J. (2009). Can bioactivity be tested in vitro with SBF solution? Biomaterials, 30(12), 2175-2179. https://doi.org/10.1016/j.biomaterials.2009.01.008

[13] Sadat-Shojai, M., Khorasani, M. T., Dinpanah-Khoshdargi, E., & Jamshidi, A. (2013). Synthesis methods for nanosized hydroxyapatite with diverse structures. Acta Biomaterialia, 9(8), 7591-7621. https://doi.org/10.1016/j.actbio.2013.04.012

[14] Kokubo, T., & Takadama, H. (2007). Simulated body fluid (SBF) as a standard tool to test the bioactivity of implants. In Handbook of Biomineralization (pp. 97-109). Wiley-VCH Verlag GmbH. https://doi.org/10.1002/9783527619443.ch51

[15] Hatano, K., Inoue, H., Kojo, T., Matsunaga, T., Tsujisawa, T., Uchiyama, C., & Uchida, Y. (1999). Effect of surface roughness on proliferation and alkaline phosphatase expression of rat calvarial cells cultured on polystyrene. Bone, 25(4), 439-445. https://doi.org/10.1016/S8756-3282(99)00192-1

[16] Einhorn, T. A., & Gerstenfeld, L. C. (2015). Fracture healing: mechanisms and interventions. Nature Reviews Rheumatology, 11(1), 45-54. https://doi.org/10.1038/nrrheum.2014.164

[17] Gergely, G., Wéber, F., Lukács, I., Tóth, A. L., Horváth, Z. E., Mihály, J., & Balázsi, C. (2010). Preparation and characterization of hydroxyapatite from eggshell. Ceramics International, 36(2), 803-806. https://doi.org/10.1016/j.ceramint.2009.09.020

[18] Ferri, J. M., Jordá, J., Montanes, N., Fenollar, O., & Balart, R. (2017). Manufacturing and characterization of poly(lactic acid) composites with hydroxyapatite. Journal of Thermoplastic Composite Materials, 31(7), 865-881. https://doi.org/10.1177/0892705717729014

[19] Marsell, R., & Einhorn, T. A. (2011). The biology of fracture healing. Injury, 42(6), 551-555. https://doi.org/10.1016/j.injury.2011.03.031

[20] Sheikh, Z., Najeeb, S., Khurshid, Z., Verma, V., Rashid, H., & Glogauer, M. (2015). Biodegradable materials for bone repair and tissue engineering applications. Materials, 8(9), 5744-5794. https://doi.org/10.3390/ma8095273

[21] Nguyen, T. T., Hoang, T., Can, V. M., Ho, A. S., Nguyen, S. H., Nguyen, T. T. T., Pham, T. N., Nguyen, T. P., Nguyen, T. L. H., & Thi, M. T. D. (2017). In vitro and in vivo tests of PLA/d-HAp nanocomposite. Advances in Natural Sciences: Nanoscience and Nanotechnology, 8(4), 045013. https://doi.org/10.1088/2043-6254/aa92b0

[22] Zhang, H., Mao, X., Du, Z., Jiang, W., Han, X., Zhao, D., Han, D., & Li, Q. (2016). Three-dimensional printed macroporous polylactic acid/hydroxyapatite composite scaffolds for promoting bone formation in a critical-size rat calvarial defect model. Science and Technology of Advanced Materials, 17(1), 136-148. https://doi.org/10.1080/14686996.2016.1145532

[23] Zulkefli, N., Yusup, E. M., & Norazam, N. M. A. (2025). Controlled Degradation in Bone Tissue Scaffolds: A Review of PCL-Enhanced PLA Composites with Naturally Derived Hydroxyapatite. International Journal of Mechanical and Sustainability Engineering Technology, 4(1), 1-12.

[24] Gilarska, A., Hinz, A., Bzowska, M., Dyduch, G., Kamiński, K., Nowakowska, M., & Lewandowska-Łańcucka, J. (2021). Addressing the osteoporosis problem—multifunctional injectable hybrid materials for controlling local bone tissue remodeling. ACS Applied Materials & Interfaces, 13(42), 49762-49779. https://doi.org/10.1021/acsami.1c17472

[25] Abdalla, M. M., Lung, C. Y. K., Neelakantan, P., & Matinlinna, J. P. (2020). A novel, doped calcium silicate bioceramic synthesized by sol–gel method: Investigation of setting time and biological properties. Journal of Biomedical Materials Research Part B: Applied Biomaterials, 108(1), 56-66. https://doi.org/10.1002/jbm.b.34365

Int. Journal of Integrated Engineering Vol. 18 No. 2 (2026) p. 82-94

[26] Wu, S. C., Hsu, H. C., Wu, W. H., & Ho, W. F. (2024). Enhancing bioactivity and mechanical properties of nano-hydroxyapatite derived from oyster shells through hydrothermal synthesis. Nanomaterials, 14(15), 1281. https://doi.org/10.3390/nano14151281

[27] Obada, D. O., Dauda, E. T., Abifarin, J. K., Dodoo-Arhin, D., & Bansod, N. D. (2020). Mechanical properties of natural hydroxyapatite using low cold compaction pressure: Effect of sintering temperature. Materials Chemistry and Physics, 239, 122099. https://doi.org/10.1016/j.matchemphys.2019.122099